

Rotational analysis of congested spectra: Application of population labeling to the BaI C-X system^{a)}

Mark A. Johnson, Christopher R. Webster,^{b)} and Richard N. Zare

Department of Chemistry, Stanford University, Stanford, California 94305
(Received 10 September 1981; accepted 1 October 1981)

Rotational analysis of the electronic spectra of heavy diatomic radicals is complicated by the large density of lines belonging to the numerous branches and bands. The alkaline earth halides, for example, have spectra in which individual lines are blended within their Doppler widths,^{1,2} frustrating conventional high-resolution techniques. One means of overcoming this problem is laser excitation spectroscopy where the molecular fluorescence is selectively detected using a monochromator or spectrograph.³⁻⁵ An alternative possibility, which only uses lasers, is the optical-optical double resonance method of lower level population labeling,⁶ in conjunction with molecular-beam Doppler reduction.^{7,8} We illustrate the power of the population labeling technique by applying it to obtain a preliminary rotational analysis of the (0, 0) band of the BaI C²Π-X²Σ* system.

Figure 1 shows a schematic diagram of the experiment. Two single-mode cw dye lasers (Coherent Model 599-21) L1 and L2, modulated at frequencies ω_1 and ω_2 , intersect a molecular beam of BaI. Laser L1 is scanned through the C₂(²Π_{3/2})-X(0, 0) rotational manifold near 538 nm, while L2 is fixed on a selected transition in the C₁(²Π_{1/2})-X(0, 0) band near 561 nm.

The resulting fluorescence from each spin orbit component of the C-X band system is detected independently by a filter-photomultiplier combination. Lock-in 1 demodulates the excitation spectrum from the scanning laser L1, while lock-in 3 monitors the fluorescence signal resulting from the fixed laser L2. Lock-in 2 records the fluorescence signal from the fixed laser L2 modulated at the chopping frequency ω_1 of L1, thereby

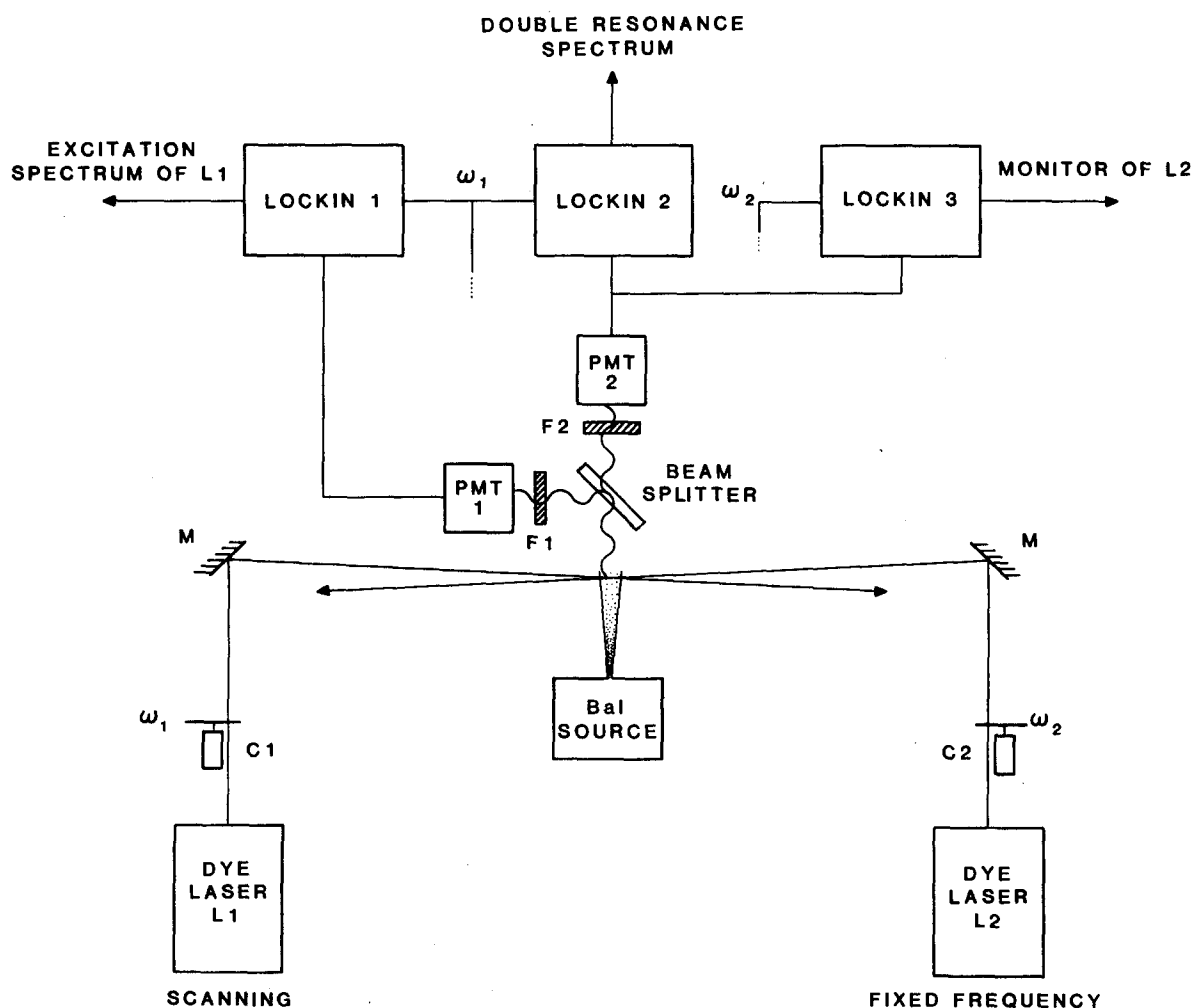


FIG. 1. Schematic of the optical-optical double resonance experiment: F=filter; PMT=photomultiplier; C=chopper; M=mirror.

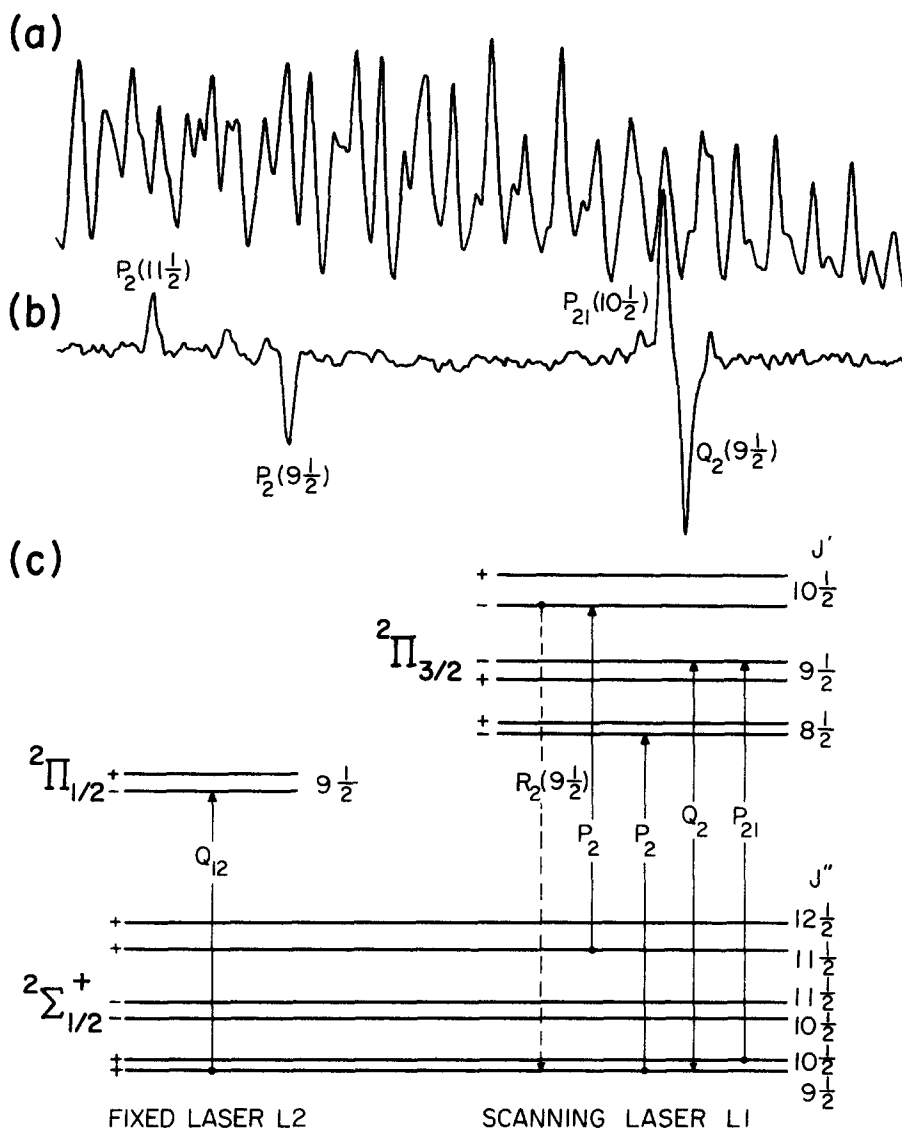


FIG. 2. Typical spectra scan (1 cm^{-1}) showing (a) the excitation spectrum from laser L1, (b) the double resonance spectrum found in the same scan as (a), and (c) the energy level diagram identifying the double resonance transitions labeled in (b).

generating the double resonance signal. Note that in this configuration, the saturating laser is scanned and the probe laser is fixed.

Figure 2 shows typical observed spectra. Figure 2(a) is a portion of the C_2-X excitation spectrum, while Fig. 2(b) is the double resonance spectrum of the same scan. The relevant level diagram is reproduced in Fig. 2(c). A double resonance signal results from a population change in the labeled level (in this case, $J'' = 9\frac{1}{2}$) probed by laser L2. Negative signals result when lasers L1 and L2 excite transitions with the same lower level, e.g., $P_2(9\frac{1}{2})$, $Q_2(9\frac{1}{2})$. Positive signals occur when L1 excites a transition terminating on an upper level optically connected to the labeled level, e.g., pump $P_2(11\frac{1}{2})$ and populate $J'' = 9\frac{1}{2}$ through fluorescence via $R_2(9\frac{1}{2})$.

With the BaI source operating at 1250 K so that $J_{\max} \approx 130$, low J lines are weak and appear usually blended with higher J lines in the excitation spectrum. However, due to the selective detection inherent in the double resonance experiment, the low J lines are readily identified [compare Figs. 2(a) and 2(b)]. Moreover, the phase relations of the double resonance lines yield direct iden-

tification of all six of the rotational branches, including the sign of the ground state spin-rotation constant, even before J assignments are made. The origin of each branch is then found by recording the double resonance spectrum for successively lower J values, permitting a complete rotational analysis of the band. Using combination differences³ between various double resonance transitions, we report the preliminary rotational constants $B_0'' = 0.02678 \text{ cm}^{-1}$ and $B_0' = 0.02670 \text{ cm}^{-1}$. A full rotational analysis of the (0, 0) band is in progress.

^{a)}The use of laser equipment from the San Francisco Laser Center and the support of the Air Force Office of Scientific Research is gratefully acknowledged.

^{b)}Present address: Jet Propulsion Laboratory, California Institute of Technology, 4800 Oak Grove Drive, Pasadena, CA 91103.

¹R. W. Field, D. O. Harris, and T. Tanaka, *J. Mol. Spectrosc.* **57**, 107 (1975).

²J. M. Brown, H. Martin, and F. D. Wayne, *Chem. Phys. Lett.* **55**, 67 (1978).

³M. Dulick, P. F. Bernath, and R. W. Field, *Can. J. Phys.*

58, 703 (1980).

⁴L. E. Berg, L. Klynning, and H. Martin, *Phys. Scr.* **21**, 173 (1980).

⁵C. Linton, *J. Mol. Spectrosc.* **69**, 351 (1978).

⁶M. E. Kaminsky, R. T. Hawkins, F. V. Kowalski, and A. L. Schawlow, *Phys. Rev. Lett.* **36**, 671 (1976).

⁷G. Höning, M. Cjalkowski, and W. Demtröder, *J. Chem. Phys.* **71**, 2138 (1979).

⁸W. J. Childs, L. S. Goodman, and I. Renborn, *J. Mol. Spectrosc.* **87**, 522 (1981).

⁹G. Herzberg, *Spectra of Diatomic Molecules* (Van Nostrand, New York, 1950), p. 262.

NOTES

A note on the transition dipole moment of alkali dimers

J. P. Woerdman

Philips Research Laboratories, 5600 MD Eindhoven, The Netherlands

(Received 11 June 1981; accepted 17 August 1981)

Recently there has been considerable interest in electronic transition probabilities of alkali dimers.¹⁻¹⁰ These probabilities are proportional to D^2 , where D is the transition dipole moment. Since alkali dimers are weakly bound molecules their value of D^2 equals roughly twice the atomic value when the correlated atomic transition is considered. It has been found from pseudopotential and *ab initio* calculations,¹⁻⁵ and from experiments,^{6,7} that D depends in fact on the internuclear distance R , typical variations being tens of percents. It is the purpose of this Note to show that for a number of alkali transitions this variation $D(R)$ is quantitatively described by the R dependence of the dimer transition frequency $\nu(R)$, assuming constant, atomic oscillator strengths [see Eq. (1)]. This aspect seems to have gone unnoticed so far.

In Figs. 1(a) and (b) the points give $D(R)$ values calculated for the $X^1\Sigma_g^+ - A^1\Sigma_g^+$ and $X^1\Sigma_g^+ - B^1\Pi_u$ transitions of Li_2 and Na_2 by Konowalow, Rosenkrantz, and Hochhauser¹ (KRH), and Stevens, Hessel, Bertoncini, and Wahl² (SHBW), using *ab initio* methods, and by Watson³ (W), and Uzer, Watson, and Dalgarno⁴ (UWD), using pseudopotential methods. Experimental data are available only for the $\text{Na}_2 X^1\Sigma_g^+ - B^1\Pi_u$ transition^{6,7}; they agree well with the SHBW calculations. The drawn curves in Figs. 1(a) and (b) represent $D(R)$ as obtained from the conventional definition of the oscillator strength [cf. Eq. (31) of Ref. 11]

$$D_{X-A}(R) = \left(\frac{3\hbar e^2}{8\pi^2 m \nu_{X-A}(R)} \frac{g_X f_{X-A}}{g_A} \right)^{1/2} \quad (1)$$

and similarly for $D_{X-B}(R)$; $\nu_{X-A}(R)$ is the $X-A$ transition frequency, g_X and g_A are the statistical weights, f_{X-A} is the $X-A$ absorption oscillator strength, and e , \hbar , and m have their usual meaning. Introducing the atomic oscillator strength F , I postulate (see discussion below)

$$f_{X-A} + f_{X-B} = 2F, \quad (2)$$

$$f_{X-B}/f_{X-A} = 2, \quad (3)$$

solve for f_{X-A} and f_{X-B} and substitute these into Eq. (1). The following numerical values have been used: $g_X = 1$,

$g_A = 1$, $g_B = 2$, $F = 0.753$ for $\text{Li } 2s - 2p$,¹² and $F = 0.982$ for $\text{Na } 3s - 3p$.¹³ $\nu(R)$ has been taken from *ab initio* Li_2 and Na_2 calculations.^{2,14,15} It is evident from Figs. 1(a) and 1(b) that Eq. (1) with the oscillator strengths defined by Eqs. (2) and (3) represents a good fit to the numerical values of $D(R)$. In particular the maximum of $D_{X-A}(R)$ is apparently associated with the minimum of $\nu_{X-A}(R)$, i.e., with the classical satellite of $X-A$. It should be noted that the agreement between the $D(R)$ data points and $D(R)$ curves in Figs. 1(a) and 1(b) is still reasonably good if the $D(R)$ curves are obtained by taking $\nu(R)$ from *experimental* potential curves.^{8,16-19} The largest differences then occur for $\text{Na}_2 X-B$, where they amount to no more than 8%. Such differences are probably not much larger than the uncertainties in the *ab initio* and pseudopotential values of $D(R)$.

Ab initio $D(R)$ and $\nu(R)$ values are also available for the transition $^3\Sigma_u^+ - ^3\Sigma_g^+$ in Na_2 and Li_2 .^{5,20,21} In this case the discrepancy with Eq. (1) is small ($\leq 6\%$) for Na_2 ; it is rather large²² ($\leq 30\%$) for Li_2 although in that case the *shape* of the $D(R)$ curve is still qualitatively well described by Eq. (1).

The good fit of Eq. (1) to $D_{X-A}(R)$ and $D_{X-B}(R)$ for Li_2 and Na_2 suggests application of Eqs. (1)-(3) to the case of K_2 , for which no theoretical or experimental $D(R)$ values are available. Substitution of $F = 1.02$ ¹³ and taking $\nu(R)$ from experimental potential curves^{23,24} yields $D(R)$ curves for K_2 shown in Fig. 1(c).²⁵

Finally, I touch briefly upon the physical implications of the apparent validity of Eqs. (2) and (3) for dimer transitions which asymptotically ($R \rightarrow \infty$) correspond with allowed atomic transitions. *A priori*, Eq. (2) is rigorously valid for $R \rightarrow \infty$ in that limit the factor of 2 is due to the fact that either the one or the other atom of the dimer can make the transition considered. Equation (2) can be approximately justified for smaller values of R by simple sum rule considerations.¹¹ Equation (3) is likewise rigorously valid for $R \rightarrow \infty$, when the dominant interatomic interaction is by resonant dipole-dipole forces. In that limit, discussed by Movre and Pichler,⁹